International Journal of Heat and Technology
Vol. 44, No. 4, August, 2026, pp. 1637-1647
Journal homepage: http://iieta.org/journals/ijht

Integrated Experimental, Exergy, and Annual TRNSYS Assessment of a Forced-Draft Counter-Flow Wet Cooling Tower under Iraqi Climatic Conditions

Doaa Zaid Khalaf[1*], Fadhil Abdulrazzaq Kareem[2], Noor Samir Lafta[2]

[1] Engineering Technical College-Baghdad, Middle Technical University, Baghdad 10074, Iraq
[2] Polytechnic College of Engineering Specializations-Baghdad, Middle Technical University, Baghdad 10074, Iraq

Corresponding Author Email: doaazaid605@gmail.com

Copyright: ©2026 The authors. This article is published by IIETA and is licensed under the CC BY 4.0 license (http://creativecommons.org/licenses/by/4.0/).

https://doi.org/10.18280/ijht.440427

Received: 12 June 2026
Revised: 2 August 2026
Accepted: 10 August 2026
Available online: 31 August 2026

Keywords:
exergy efficiency, thermal efficiency, exergy destruction, TRNSYS, ambient wet-bulb temperature

ABSTRACT

The performance of wet cooling towers under hot and seasonally varying Iraqi climatic conditions cannot be adequately evaluated using thermal analysis alone, because improved heat rejection may be accompanied by increased thermodynamic irreversibility. Hence, this study combines experimental testing, exergy analysis, and annual TRNSYS simulation for a comprehensive evaluation of a forced-draft counter-flow wet cooling tower. The inlet water temperatures ranged from 28 °C to 42 °C and water mass flow rates from 0.03 to 0.075 kg/s, with the first and second laws of thermodynamics used to capture the thermal performance and exergy losses. The results indicated that the cooling range and thermal efficiency increased with the increase in inlet water temperature and water mass flow rate, and the maximum values of the cooling range and the thermal efficiency were 14.8 °C and 74%, respectively. However, this heat-rejection enhancement has been accompanied by an increase in the exergy destruction from about 1.0 kW to 2.8 kW, and a decrease in the exergy efficiency from 57.8% to 11.9%, which is a clear trade-off between heat-rejection enhancement and exergy losses due to irreversibilities in the system. The maximum cooling capacity achieved by the annual simulation of TRNSYS was 4.8 kW and was within the range of 5.6% error from the experimental results. The integrated approach gives a practical approach to select operating points that minimize cooling performance and exergy loss, and helps the optimization of wet cooling towers in Iraqi climatic conditions.

1. INTRODUCTION

In a cooling tower, heat and mass are transferred from the air to the water, which is a form of a heat exchanger. Cooling towers are used in air conditioning systems, refrigeration, industrial power plants, and chemical industries to accommodate a significant heat load of up to 325 kW [1, 2]. Supply hot water is sprayed into tiny water droplets by a nozzle, which is then sprayed onto the packaging material. This process helps increase the evaporation rate of the water and lowers the temperature of the water [3]. Cooling towers can be categorized as forced-draft, natural draft, counter-flow, and cross flow, due to the air and water flow [4]. As stated by the first law of thermodynamics, it does not reveal the location or amount of energy loss. As a result, exergy has become a popular unit of measurement among scientists in recent years. The maximum amount of work that can be accomplished while maintaining equilibrium with the environment is known as exergy. Additional information is provided by the exergy analysis of thermal systems. Theoretically, according to Muangnoi et al. [4], the cooling tower's water and air flow's thermodynamic properties may be predicted. While the water exergy was lower at the bottom of the cooling tower than on the top side, the exergy of humid air was higher than it was on the top side. A theoretical model was created by Ataei et al. [5] to assess the cooling tower's air and water parameters. Experimental data were used to validate the computer model's predictions. The data showed that the water-energy clearly increased from the bottom to the top of the cooling tower. The cooling tower effectiveness and the applicability of the second rule both decline when the flowing water temperature through the cooling tower rises, along with the energy losses. Khalifa [6] to generate measures of mass, energy, and exergy, used an engineering equation to solve geometric equations. Although it seemed as though the excessive energy destruction of water in the cooling tower bottom was less than that at the tip, the destruction of air was more. As moisture content rises, chemical energy does too, while thermal energy falls. The cooling tower was simulated using computers by Akbarpour Ghazani et al. [7]. The data showed that as the water level dropped from the tower top to its bottom, the air energy increased while the energy of the water declined. The general air energy exhibited the same pattern as the chemical energy. A two-dimensional digital model was produced using MATLAB [8]. The experimental values used to validate the numerical model were taken from the previous research. The information demonstrated that when the incoming water's temperature dropped, the cooling tower's efficiency rose. The highest efficiency was 55.28% when the temperature of the water was close to 36 °C. Kareem et al. [9] studied the cooling

tower performance in terms of energy and exergy. The exergy destruction increased from top to bottom in the cooling tower, whereas the exergy efficiency, thermal exergy, and exergy destruction of air all decreased from the top to the bottom. Counter-flow wet cooling towers' energy and exergy are assessed using the Engineering Equation Solver. The performance and efficiency of cooling towers are strongly influenced by the wet bulb temperature of the incoming air. In thermal power plants, the mass flow rate ratio of water to air is 2.47 and 2.09, respectively, and the ratio fluctuates based on the wet-bulb temperature of the entering air. This investigation by Fan et al. [10] concluded that the wet-bulb temperature was to blame for the results. Recent studies have focused on improving the thermal and exergy performance of cooling towers through advanced designs, optimization techniques, and numerical modeling. Ruiz et al. [11] experimentally investigated a novel mechanical-draft wet cooling tower and reported improved thermal performance compared with conventional designs. Qu et al. [12] suggested a bi-level reduced-order modelling method to optimize the exergy performance of a closed-wet cooling tower with weather changes. Data-driven and physics-based reduced order models were developed using multi-sample computational fluid dynamics (CFD) simulations, principal component analysis, and an artificial neural network. The developed approach enabled the simultaneous determination of the optimum exergy-efficiency ratio and the spatial distributions of thermal, mechanical, and chemical exergy fluxes with substantially lower computational requirements than full CFD optimization. The study pointed out the benefits of reduced order models for fast thermodynamics optimization of a cooling tower system. Li et al. [13] numerically studied the heat and mass transfer characteristics of a wet cooling tower equipped with optimized baffle configurations and demonstrated enhanced cooling performance and more uniform temperature distribution. Chen et al. [14] numerically investigated the use of wind shields to mitigate the adverse effects of crosswinds on the thermal performance of mechanical-draft wet cooling towers. The wind shields proposed forced the flow velocity and water temperature to be more uniform and reduced transverse vortices. The water-temperature drop was recovered by 17.2% and 9.4% and the ventilation rate increased by 33.1% and 19.5% for the single- and double-air-inlet cooling towers, respectively, at a crosswind angle of 90° and a velocity of 10 m/s. These results showed the effectiveness of the structural modification to enhance the performance of the cooling tower in adverse wind conditions. Yang et al. [15] developed and validated a three-dimensional numerical model to optimize the thermal performance of a large natural-draft wet cooling tower through the simultaneous modification of the water-spraying, fill, and rain zones. The proposed optimization involved the use of partitioned water distribution, non-equidistant fill arrangement, and the use of a dry-wet hybrid rain zone. The optimized configuration was compared with the conventional one without optimization; the water-temperature drop was raised by 0.58 ℃, the cooling efficiency was enhanced by 3.37%, the Merkel number by 0.17, and the ventilation rate by 1480 kg/s. The results showed that a multi-zone synergistic optimization is more effective than optimizing one zone of heat- and mass-transfer zone at a time. Bueso et al. [16] used TRNSYS to simulate a cooling tower in a ZLD desalination process. More than 12,000 simulated data points were generated and used to train a multilayer perceptron model for estimating the evaporated water mass. The developed model showed a coefficient of determination of about 0.76 and was more successful in predicting the model than the conventional linear regression model. The sensitivity analysis they performed also showed that their inlet brine temperature was one of the most important factors affecting the amount of evaporated water.

Qu et al. [17] developed a comprehensive coupled model incorporating the spray, packing, and rain zones of a counter-flow seawater cooling tower and evaluated its performance from both energy and exergy perspectives. The total water exergy loss increased by 5.86 to 15.62% and the exergy efficiency decreased by 3.52 to 10.72% when the seawater salinity increased from 35 g/kg to 105 g/kg. Furthermore, the outlet-water temperature increased by 1.08–3.60%, whereas the cooling efficiency and overall heat dissipation decreased by 2.29–7.59% and 4.18–13.41%, respectively. The study highlighted that proper operating conditions were crucial to reduce the exergy destruction and enhance the cooling performance. Zhou et al. [18] used experimental tests and numerical simulation to optimize the geometry of heat-transfer tubes for a closed-circuit cooling tower. They proposed an optimized deflected elliptical-tube arrangement and examined its performance under different air velocities and spray-water flow rates. In the optimized layout, the heat transfer coefficient was raised by 16.27% (with air velocities of 2 to 3.2 m/s) over the conventional layout. Moreover, the proposed geometry decreases the total volume of the heat-exchanger unit by 24.03%, which shows the possibility of increasing the thermal efficiency and reducing the consumption of materials.

Deng and Sun [19] examined a mechanical-draft wet cooling tower fitted with a condensation-plume module and performed a multi-objective optimization based on cooling performance, water conservation, and plume-abatement requirements. Their investigation showed that the parameters that lead to better water recovery and to lower visible plumes could also have an impact on the heat rejection capability of the tower. Thus, the authors set up a framework for optimization to determine the appropriate operating conditions to give a good balance of thermal performance, water-saving capability, and plume control. Luo et al. [20] conducted a comprehensive energy-exergy-environmental assessment of a shower cooling tower and demonstrated considerable potential for reducing exergy destruction through operational optimization. Recent developments in CFD and numerical modelling have also provided valuable insights into the coupled heat and mass transfer mechanisms occurring inside wet cooling towers, enabling more accurate performance prediction and optimization under varying climatic conditions. Experimental investigations are usually used in a limited operating range of the cooling tower, a short period of testing, and under controlled ambient conditions to validate the theoretical and numerical predictions of cooling-tower performance; they have this drawback. Mathematical and thermodynamic models are useful for describing overall heat and mass transfer and identifying exergy losses, but their accuracy depends on simplifying assumptions and empirical correlations. CFD methods can give detailed spatial information of the airflow, the temperature, the humidity, and local heat- and mass-transfer mechanisms, but are typically very demanding in terms of computation and are often used under specific operating conditions or geometric configurations. The transient modeling and evaluation of long-term performance under continuously changing meteorological conditions, however, is possible with

TRNSYS, but the results must be validated by experiments to verify the applicability to the cooling tower investigated and the local climate. Thus, none of these methods can be used to fully assess real performance, thermodynamic irreversibility, and annual climatic response. The purpose of the present study is to overcome these complementary limitations; the study was carried out using a forced-draft counter-flow wet cooling tower in Iraqi climatic conditions with actual controlled experimental tests, exergy analysis, and annual TRNSYS simulation. Despite the progress achieved by these individual approaches, limited studies have integrated experimentally validated thermal measurements, exergy evaluation, and annual transient simulation for forced-draft counter-flow wet cooling towers operating under Iraqi climatic conditions. Thus, the current study will apply such an integrated approach to assess the actual performance, to calculate thermodynamic irreversibility, and to foresee seasonal fluctuations in cooling capacity, in order to have a more holistic foundation for cooling-tower optimization.

2. COOLING TOWER DESCRIPTION

Figure 1 depicts the experimental setup of cooling tower setup employed in the current study. The device has a cross-section of 200 × 200 mm and a length of 800 mm. 12 cm of packing fill is used. An axial fan moves air up and down the cooling tower. The water on the filling is spread by a centrifugal pump. The incoming water is heated by two heaters (0.5 and 1 kW each). A flow meter and a manometer are attached to the discharge side to measure the water and airflow rates. The air and water temperatures are measured using six type-K thermocouples. At the intake and outflow, four sensors monitor the air DBT and WBT, while the other sensors measure the water temperature. The cold water can be collected in a basin at the device bottom, which is used to measure its temperature. Table 1 shows the cooling tower specifications and measurement uncertainty.

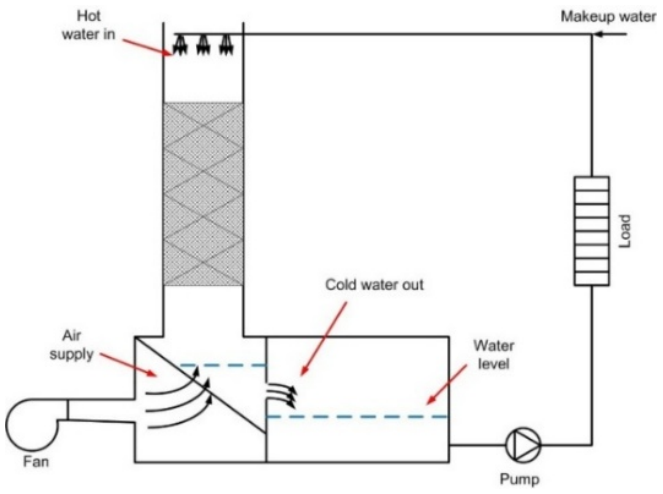


Figure 1. Experimental set-up

During all experiments, the inlet-air dry-bulb temperature and relative humidity were maintained at approximately 27 ℃ and 60%, respectively, corresponding to an inlet-air wet-bulb temperature of approximately 21.3 ℃. With the axial fan running constantly at the same fixed position to create the same air-side conditions for all tests, the water inlet temperature and mass flow rate were adjusted. There is no independent recording of the fan power, rotational speed, and calibrated airflow rate, which is considered a limitation in the experimental characterization.

Table 1. Cooling tower specification

Component	Specification
Tower cross-section	200 × 200 mm
Tower length	800 mm
Fill thickness	120 mm
Fill material	Packing fill
Fan type	Axial fan
Heater power	0.5 and 1 kW
Total heating capacity	1.5 kW
Pump type	Centrifugal pump
Instrument	Accuracy
Thermocouple	±0.5 ℃
Flow meter	±2%
Manometer	±1%

All the operating conditions with different inlet water temperatures and mass flow rates were conducted under three independent conditions. A steady state was achieved in the cooling tower before data collection by operating the tower for around 20 min. The inlet- and outlet-water temperatures, and the inlet-air dry- and wet-bulb temperatures were seen to be in the range of ±0.5 ℃ with the water mass flow rate in the range of ±2% for a minimum duration of 10 minutes. Once in steady state, the variables measured were taken at 1 min intervals for 15 min. The values reported in the manuscript represent the averages of the three independent runs, and measurement variability was evaluated using the standard deviation.

3. METHODOLOGY

The mass of the evaporated water through the cooling tower into the air, as seen in Figure 2, can be calculated by Navarro et al. [3].

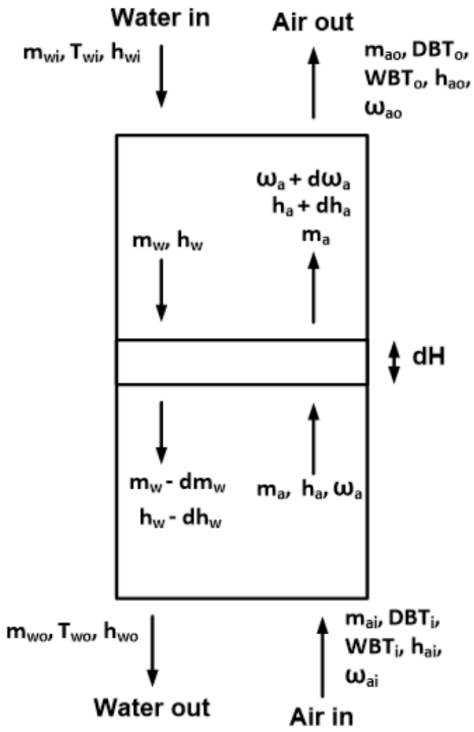


Figure 2. The test rig control volume

$$d\dot{m}_v = \dot{m}_a * d\omega \quad (1)$$

The heat balance can be expressed as:

$$\dot{m}_a * dh_a = h_{f,w} * \dot{m}_a * d\omega + m_w * dh_{f,w} \quad (2)$$

$$dh_{f,w} = cp_w * dT_w \quad (3)$$

$$dT_w = \frac{\dot{m}_a}{\dot{m}_w * cp_w} * \left(dh_a - h_{f,w} * d\omega\right) \quad (4)$$

The cooling range, which is defined as the variation in temperature of the water between both the entrance and exit streams, is one measure that can be used to describe how well the wet cooling tower performs [7].

$$R = T_{wi} - T_{we} \quad (5)$$

The heat transfer from water to the airflow is what is meant by cooling capacity [21].

$$Q = \dot{m}_w * cp_w * (T_{wi} - T_{we}) \quad (6)$$

Cooling tower efficiency can be estimated by [21]:

$$\eta = \frac{(T_{wi} - T_{we})}{(T_{wi} - WBT_i)} \quad (7)$$

The cooling range represents the actual reduction in water temperature as it passes through the cooling tower, whereas the cooling capacity quantifies the rate of heat removed from the circulating water. The thermal efficiency is the ratio of the actual amount of water-temperature reduction to the maximum possible reduction, which is limited by the inlet-air wet-bulb temperature. The first law parameters are the magnitude of the heat transfer and the cooling efficiency of the tower, but they do not reveal degradation of energy quality or irreversibilities from simultaneous heat and mass transfer.

The exergy analysis is used to complement the first law evaluation, which measures the maximum useful work that can be provided by the water and humid-air streams relative to the environmental reference state. The exergy of humid air includes thermal and chemical contributions arising from differences in temperature and humidity ratio, while the water and vapor exergies represent their useful-work potentials relative to the dead state. Thus, the exergy terms reflect not only the amount of energy transferred, but also the quality of the transferred energy.

The exergy for the cooling tower can be divided into the following categories for a steady-state flow:

1. The humid air exergy

The humid air exergy involves convective and evaporative exergy of heat transfer. Can be presented as [10].

Convective heat transfer exergy

$$Ex_{a,c} = \dot{m}_a * \begin{bmatrix} cp_a * (T_a - T_o) - T_o * cp_a * ln\left(\frac{T_a}{T_o}\right) + \\ \omega_a * \left(cp_v * (T_a - T_o) - T_o * cp_v * ln\left(\frac{T_a}{T_o}\right)\right) \end{bmatrix} \quad (8)$$

Evaporative heat transfer exergy

$$Ex_{a,e} = \dot{m}_a * \begin{bmatrix} R_a * T_o * ln\left(\frac{1 + 1.608 * \omega_{a,o}}{1 + 1.608 * \omega_a}\right) + \\ \omega_a * R_v * T_o * ln\left(\frac{\omega_a * (1 + 1.608 * \omega_{a,o})}{\omega_{a,o} * (1 + 1.608 * \omega_a)}\right) \end{bmatrix} \quad (9)$$

2. The water exergy

The water exergy can be represented as [22]:

$$Ex_w = (h_w - h_{w,o}) - T_o * (s_w - s_{w,o}) - R_v * T_o * ln\, \emptyset_o \quad (10)$$

3. Exergy of vapor

At the water temperature, vapor's exergy is determined by [10]:

$$Ex_w = cp_v * (T_w - T_o) - T_o * cp_v * ln\left(\frac{T_w}{T_o}\right) + R_v * T_o * ln\,(\emptyset_o) \quad (11)$$

4. Exergy destruction

The total exergy destruction can be determined by [7, 13]:

$$Ex_{dest.} = \sum Ex_{in} - \sum Ex_{out} \quad (12)$$

5. Exergy efficiency

The cooling tower second law efficiency can be expressed as [10]:

$$\eta_{ex} = \frac{Ex_{out}}{Ex_{in}} \quad (13)$$

Exergy destruction represents the loss of useful-work potential caused by thermodynamic irreversibilities, including heat and mass transfer across finite temperature and concentration differences, water-air mixing, evaporation, and flow resistance. The Gouy-Stodola principle states that the exergy destruction is proportional to the entropy generation. The ratio of exergy in the total outlet to exergy in the total inlet is called exergy efficiency and represents the portion of exergy supplied that is available at the end of the cooling process. Therefore, in the case of similar inlet conditions, a higher amount of exergy destruction increases the amount of exergy that cannot be recovered from the outlet, and in general, it decreases the exergy efficiency. Thus, the first- and second-law analyses must be used together as there can be significant irreversibility and degradation of energy quality even if the system is thermally efficient.

4. NUMERICAL MODEL

For complicated transient system simulations, TRNSYS is meant to break down the issue into several smaller components known as types [23]. The performance of the cooling tower was theoretically analyzed using TRNSYS 18.1 software within a step time of one hour under the conditions of Iraq-Baghdad, 33.3° N latitude, 44.14° N longitude, and elevation of 34 m. The schematic diagram of the developed model, shown in Figure 3, consists of the following components: The ambient temperature from Metronome for Baghdad city in Iraq.

1. Weather data
2. The water tank
3. The circulation pumps

4. Auxiliary heater
5. Cooling tower
6. Psychrometric
7. Output

Table 2 illustrated these component types in TRNSYS. The geometric dimensions and operating conditions of the experimental cooling tower, such as tower dimensions, packing depth, inlet-water temperature, water mass-flow rate, and auxiliary-heater capacity, were measured and used to determine the TRNSYS model parameters. The experimental results were not used to calibrate or tune the TRNSYS model. These were, however, only for independent model validation. The model was initially created based on the physical description of the test rig and the standard formulations that were used in the TRNSYS components. Subsequently, the numerical cooling capacity was calculated under operating conditions corresponding to the experimental tests and compared with the measured heat-transfer rate. The relative deviation was calculated by dividing the numerical value by the experimental value. The obtained deviation of 5.6% was found acceptable and validated the application of the model for the annual simulation under the climatic conditions of Baghdad.

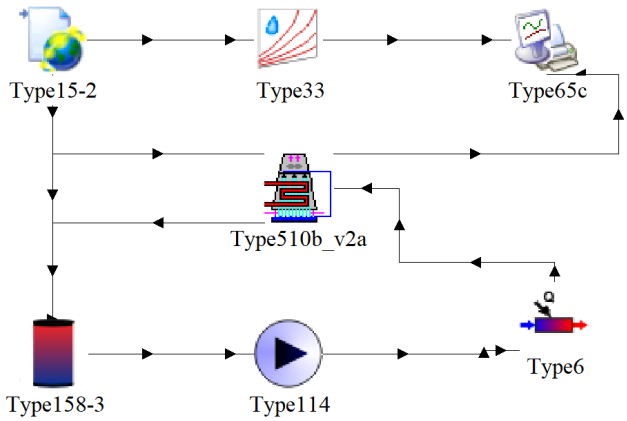


Figure 3. The schematic diagram of the developed model in TRNSYS simulation studio

Table 2. TRNSYS types used

Component	Type Number
Weather data	Type15-2
The water tanks	Type158-3
The circulation pumps	Type114
Auxiliary heater	Type6
Cooling tower	Type510b_v2a
Psychrometric	33
Output	Type65c

The TRNSYS model was developed to represent the geometry and operating range of the experimental forced-draft counter-flow wet cooling tower. The Type510b_v2a cooling-tower component was parameterized based on the experimental tower with a cross-section of 0.20 × 0.20 m, a tower height of 0.80 m, and a packing-fill depth of 0.12 m. The mass flow rates of water used were 0.03, 0.05, and 0.075 kg/s, and the water inlet temperature was changed from 28 to 42 °C based on experimental test conditions. These were represented by the circulation pump (Type114), the water-storage tank (Type158-3), and the auxiliary heater (Type6) with the installed total heating capacity of 1.5 kW. Data for hourly weather were imported at 33.3° north latitude, 44.14° east longitude, and 34 m above sea level for the city of Baghdad in Iraq with a time step of 1 hour for Type15-2. The meteorological variables used to define the inlet-air condition were transferred to the Type33 psychrometric component, which calculated the corresponding wet-bulb temperature and humidity properties of the air. These outlet water properties (calculated in the above-mentioned method), along with the inlet water temperature and water mass-flow rate, were fed to Type510b_v2a to calculate the outlet water temperature and cooling capacity. The hourly results were recorded and displayed for the entire period of the annual simulation using Type65c. The heat transfer rate of the developed model was compared with that of the experimental value, and the difference was around 5.6%, which showed good agreement in the annual performance evaluation of the model.

5. RESULTS AND DISCUSSION

Experimental and exegetical research was conducted on the wet cooling tower's functioning. In the investigations, the flow rates were selected at three values of 0.03, 0.05, and 0.075 kg/s, with water input temperatures ranging from 28 to 42 degrees Celsius; the relative humidity was kept constant at 60 percent, and the outside temperature was kept at 27 degrees Celsius. In varied mass flow rates of water, the relationship between the cooling tower's thermal efficiency and water temperature is depicted in Figure 4. The cooling tower is more effective at dissipating heat when the water temperature is higher. As the water flow rate rises, so does the thermal efficiency, as seen in the figure. 0.03, 0.05, and 0.075 kg/s each enhance the thermal efficiency from 0.43 to 0.69, 0.51 to 0.71, and 0.6 to 0.74. There is less impact on thermal efficiency when the water temperature is lower than it is when the flow rate is higher.

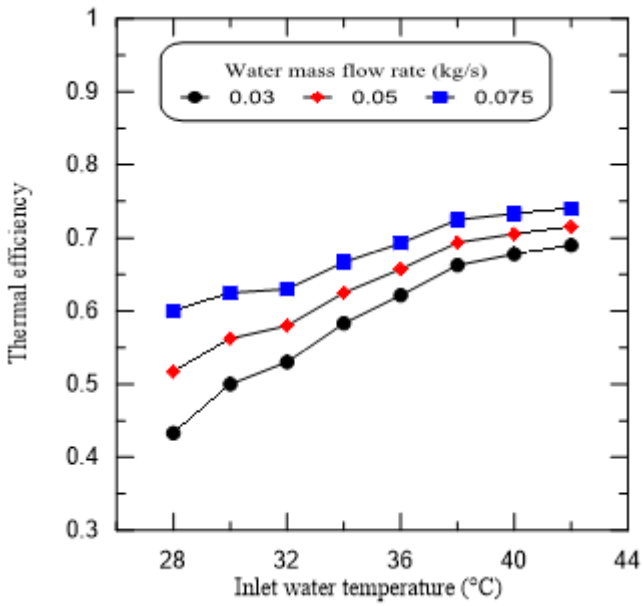


Figure 4. Thermal efficiency of the cooling tower

Figure 5 demonstrates how the cooling area fluctuates with the temperature of the entering water at varied water flow rates. It is worth mentioning that as the entering water temperature rises, cooling range likewise increases. Cooling range is governed by the quantity of heat produced and the

pace at which the water circulates. The cooling range does not alter if both the water pump speed and the heat load remain constant. For the three flow rates that were selected, the average ranges are 8.2, 8.7, and 9.2 ℃, respectively.

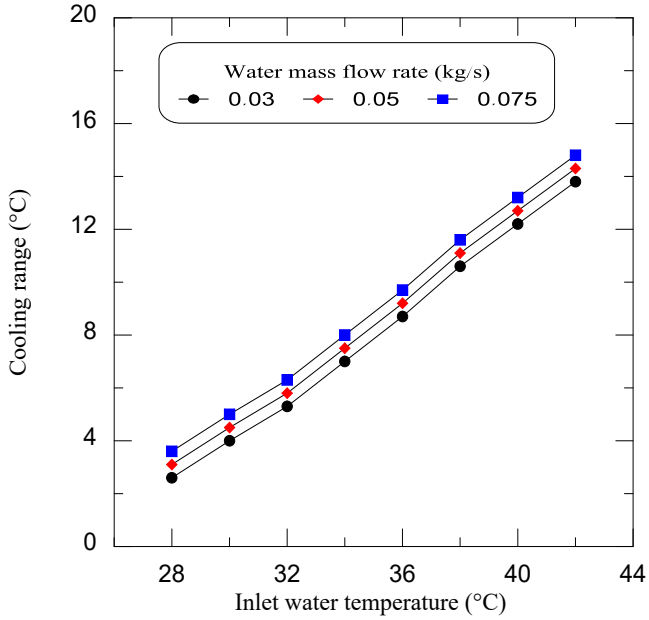


Figure 5. The cooling tower range

The observed improvements in thermal efficiency and cooling range can be understood through the coupling of heat and mass transfer between the water and air streams. When the hot water is sprayed on the packing material, it will be broken down into droplets and thin films, creating an increased air-water contact area. As a result of the temperature difference, sensible heat is transferred from water to air, and some of the water also evaporates and transfers latent heat to the air flow. The higher the inlet-water temperature, the higher the saturation vapor pressure at the surface of the water and the larger the difference between the vapor pressure and the humidity ratio of the water surface and the bulk air. This results in an increase in evaporation intensity and the total heat-transfer rate, hence more reduction in water temperature. The relatively cool unsaturated air enters the tower at the bottom and meets the downward flowing water in the counter-flow arrangement. The temperature of the air rises as it ascends, but the moisture content rises, and the temperature of the water gradually falls. The opposite flow arrangement will keep the temperature and humidity driving forces constant throughout the packing height. The wet-bulb temperature of the inlet air is the minimum possible temperature that the outlet water could attain. Thus, as the water inlet temperature increases for any given wet-bulb temperature, the water temperature minus the wet-bulb temperature increases and will increase sensible cooling and evaporation. This mechanism is why cooling range and thermal efficiency have increased, as shown in Figures 4 and 5. The higher the water mass flow rate, the more water thermal energy that will be transferred to the tower and the more water that will be spread across the packing surface. This enhances the heat-removal rate and air–water contact in the investigated range. The effect of water flow rate, however, will be affected by the liquid to gas flow-rate ratio, packing characteristics, and contact time, and too high a water flow rate will eventually limit the cooling due to the fact that the airflow may no longer be capable of absorbing the extra heat and moisture.

Figure 6 displays the wet air moving exergy, which includes the convection and evaporation exergy. Exergy differential rises with water temperature due to convective heat and mass transport. The exergy difference between air and water is insignificant at low water temperatures, suggesting that neither the air nor the water is heated. The amount of water that has evaporated has an impact on the air exergy difference, while the amount of water that is flowing does not. Consequently, the exergy difference of the air is only slightly affected by the water flow rate. For the three flow rates that were selected, the average exergy of the air is 0.144, 1.45, and 0.17 kW, respectively.

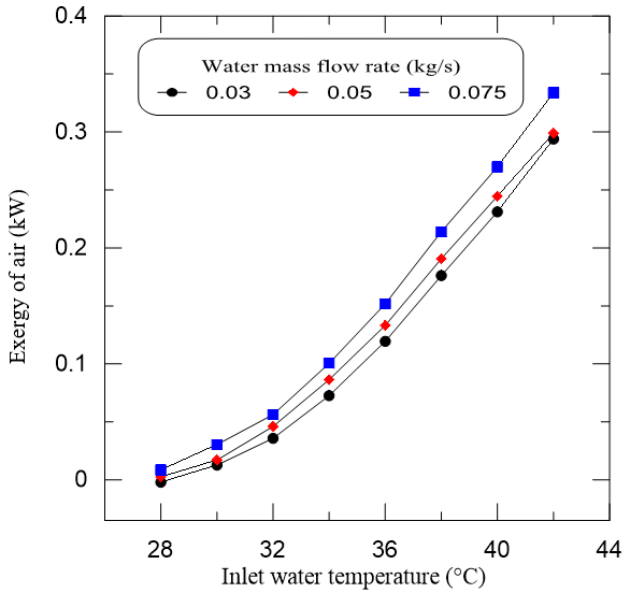


Figure 6. The exergy of humid air

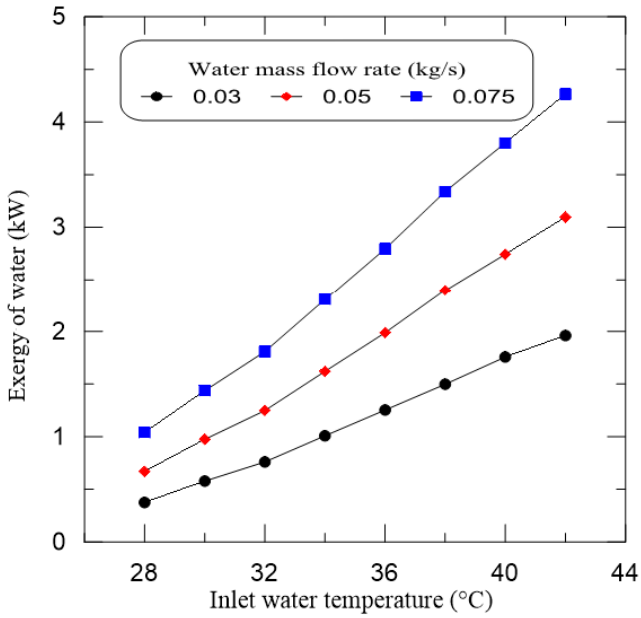


Figure 7. The exergy of water

Figure 7 shows that the exergy of water builds up as the temperature and flow rate of the incoming water are raised. The higher the temperature of the incoming water, the more it deviates from the dead state, and the higher the exergy level. For the three flow rates selected, the average exergy of water

is 1.16, 1.87, and 2.64 kW, respectively.

The vapor exergy is seen in Figure 8. Increasing the water temperature increases vapor exergy, as can be shown. As the temperature rises, so does the quantity of water that evaporates. The vapor's exergy is also generally stable, regardless of variations in water flow rate. For the three flow rates that were selected, the average exergy of vapor is 0.01375, 0.01295, and 0.013 kW, respectively.

Figure 9 demonstrates the total exergy destruction depending on the flow and temperature of the water. Incoming water with a greater temperature has a higher potential, which means more exergy is lost. For the three flow rates that were selected.

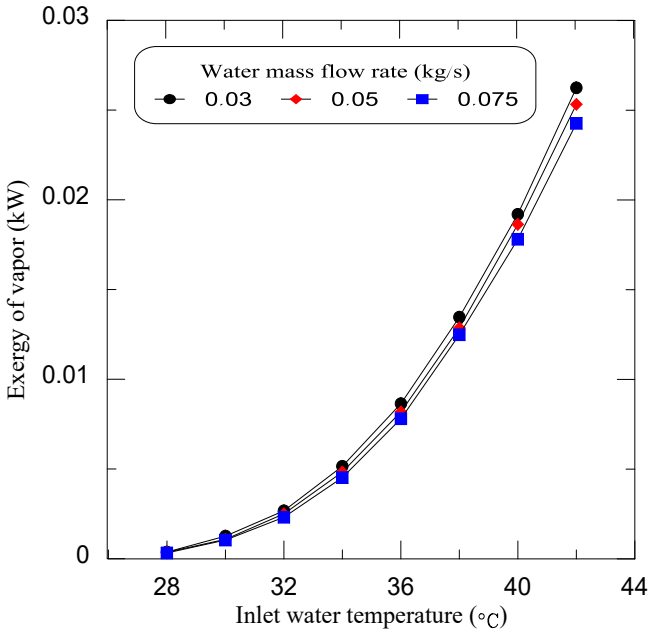


Figure 8. Exergy of the vapor

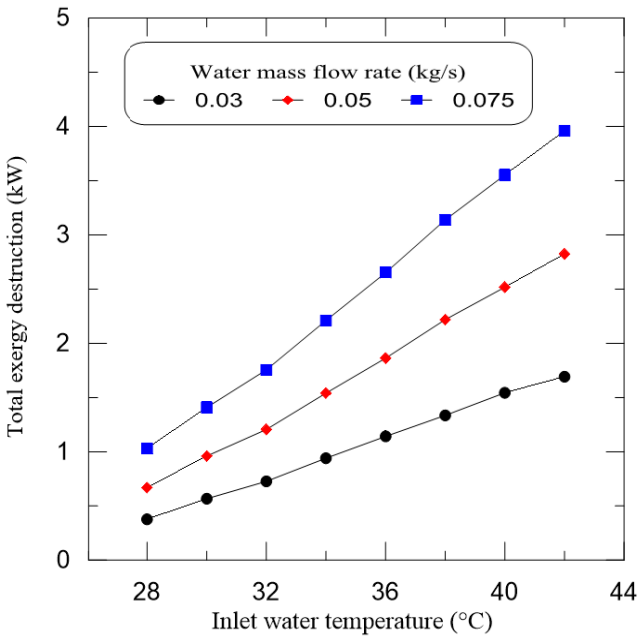


Figure 9. Total exergy destruction

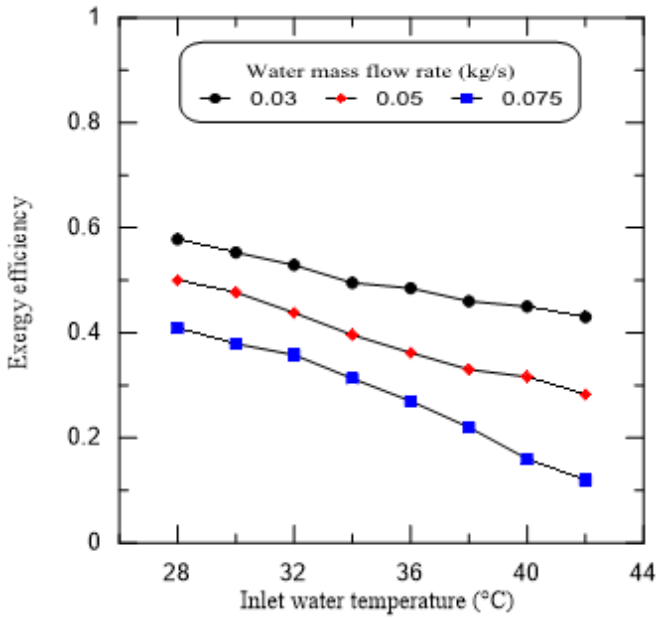


Figure 10. The cooling tower exergy efficiency

Figure 10 demonstrates the exergy efficiency as a function of the temperature of the incoming water for different water flow rates. When the incoming water temperature and flow rate were increased, the exergy efficiency decreased. This is because the greater the exergy destruction, the lower the exergy efficiency. For the three flow rates that were selected, the exergy efficiency dropped from 0.578 to 0.43, 0.501 to 0.2827, and 0.409 to 0.119, respectively. The exergy trends are also directly related to the intensification of the air–water interaction. The water inlet temperature and mass flow rate affect the thermal and physical exergy of the water stream. Concurrently, there are higher temperature and humidity disparities between the water and air surfaces, which improve heat transfer, evaporation, and mixing. These mechanisms provide for the increased cooling range and thermal efficiency, but are associated with increased entropy due to transfer of heat and mass over finite temperature and concentration differences. Consequently, a larger portion of the inlet exergy is destroyed by irreversibility. The moist air acquires thermal and chemical exergy due to its temperature and moisture content, while the water stream loses thermal exergy as it gets cooler and evaporates. The resulting rise in useful outlet exergy is, however, less than the rise in exergy destruction that occurs at the higher operating conditions. This is why the thermal efficiency can go up and the exergy efficiency down. Thus, the results prove that a higher rate of evaporation leads to a higher heat rejection rate, but it also increases thermodynamic irreversibility, which shows the importance of conducting analysis of the tower from both energy and exergy perspectives. Among the evaluated exergy components, the water stream exhibited the largest exergy magnitude and the strongest sensitivity to water inlet temperature and mass-flow rate. On the other hand, the exergy of humid air was significantly smaller, and the exergy of vapor made the least contribution. Thus, the improvement of the total exergy destruction was primarily attributed to the degradation of the water-side thermal exergy due to the heat and mass transfer, which increased with the rise of water inlet temperature and water mass-flow rate.

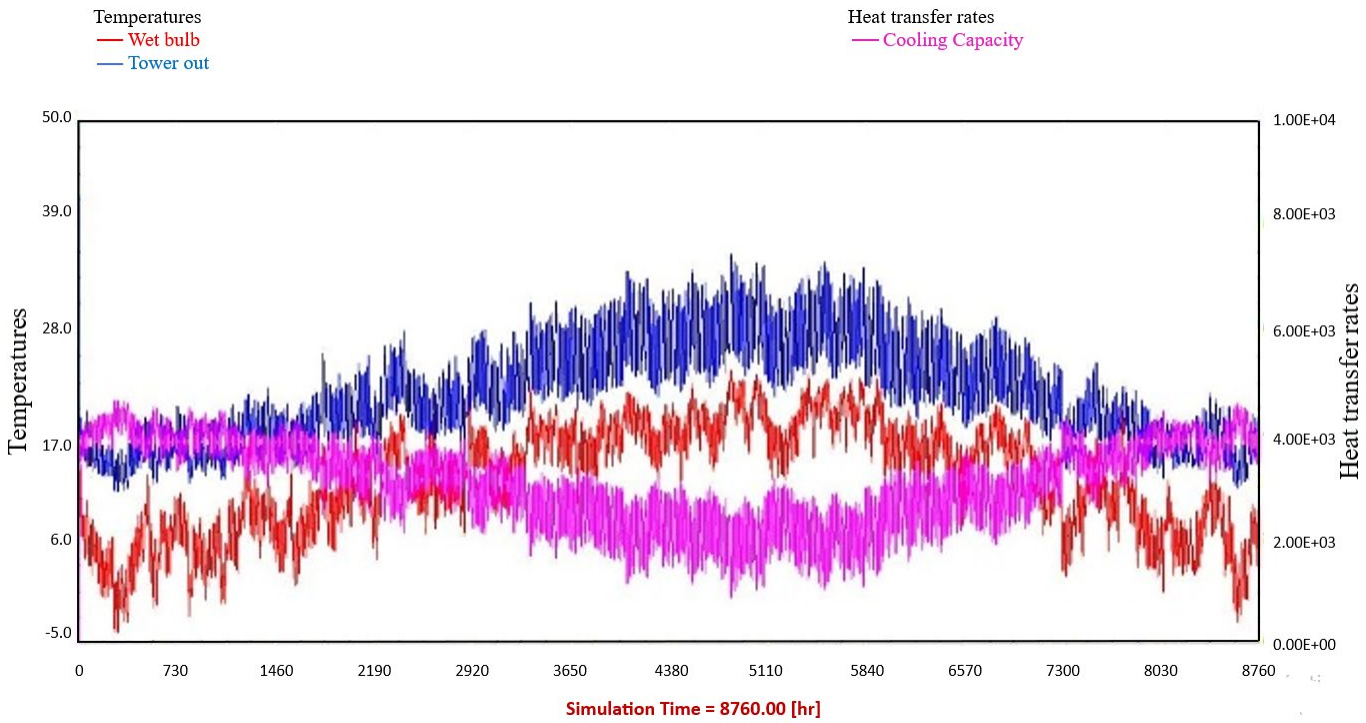


Figure 11. Variation of the outlet water temperature, wet bulb ambient temperature, and cooling capacity

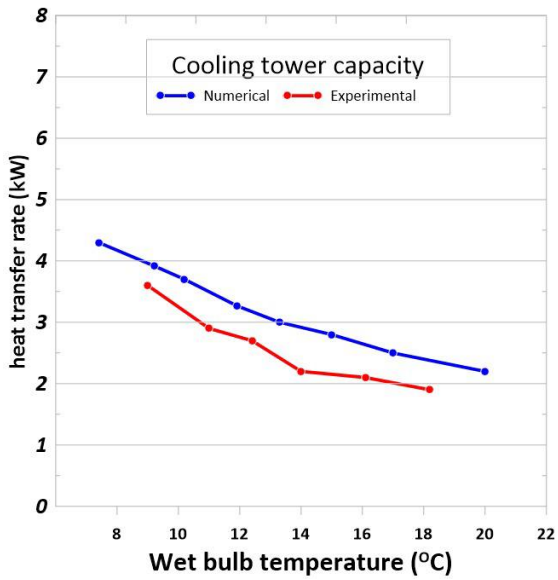


Figure 12. The validation between numerical and experimental heat transfer rate

Figure 11 shows the TRNSYS simulation results for one year. It can be seen that the heat transfer rate reaches 4.8 kW in a cold climate and decreases to 1 kW as the ambient temperature increases. The findings show that there is a greater difference in cold weather than in warm weather between the cooling tower output water temperature and the wet-bulb ambient temperature. Thus, the cooling tower is more efficient in warm climates than in cold climates because the maximum water outlet temperature that the cooling tower can reach is equal to the wet-bulb temperature of the environment. To validate the developed TRNSYS model independently, the simulated cooling capacity was compared with the experimental heat-transfer rate under corresponding operating conditions. The model parameters were not adjusted using an experimental value. The numerical prediction has shown the same value as the experimental value, as shown in Figure 12, and there is an acceptable agreement between the two approaches.

To provide a broader context for the present results, Table 3 compares the thermal and exergy performance of the investigated cooling tower with selected previous studies. The comparison is not meant to provide a precise ranking of the different systems, and it should be used to show general performance trends and differences in methodology, since the various systems are differently configured, with different operating conditions, different measurement procedures, and different thermodynamic formulations.

Table 3. Qualitative comparison with previous cooling-tower studies

Study	Configuration and Method	Reported Performance	Comparison Note
[7]	Laboratory counter-flow wet tower; experimental energy-exergy analysis	Thermal: 68%; Exergy: 32%	Different geometry and operating conditions
[9]	Forced-draft wet tower; experimental exergy analysis	Thermal: 71%; Exergy: 28%	Different operating range and calculation method
[21]	Natural- and forced-draft wet towers; experimental and numerical analysis	Thermal performance evaluated	Exergy performance was not reported
[22]	Counter-flow wet tower; theoretical parametric analysis	Exergy performance evaluated	Different model assumptions and exergy formulation
Present work	Forced-draft counter-flow wet tower; experiment, exergy, and TRNSYS	Thermal: 74%; Exergy: 57.8%	Specific to the present system and Iraqi climate

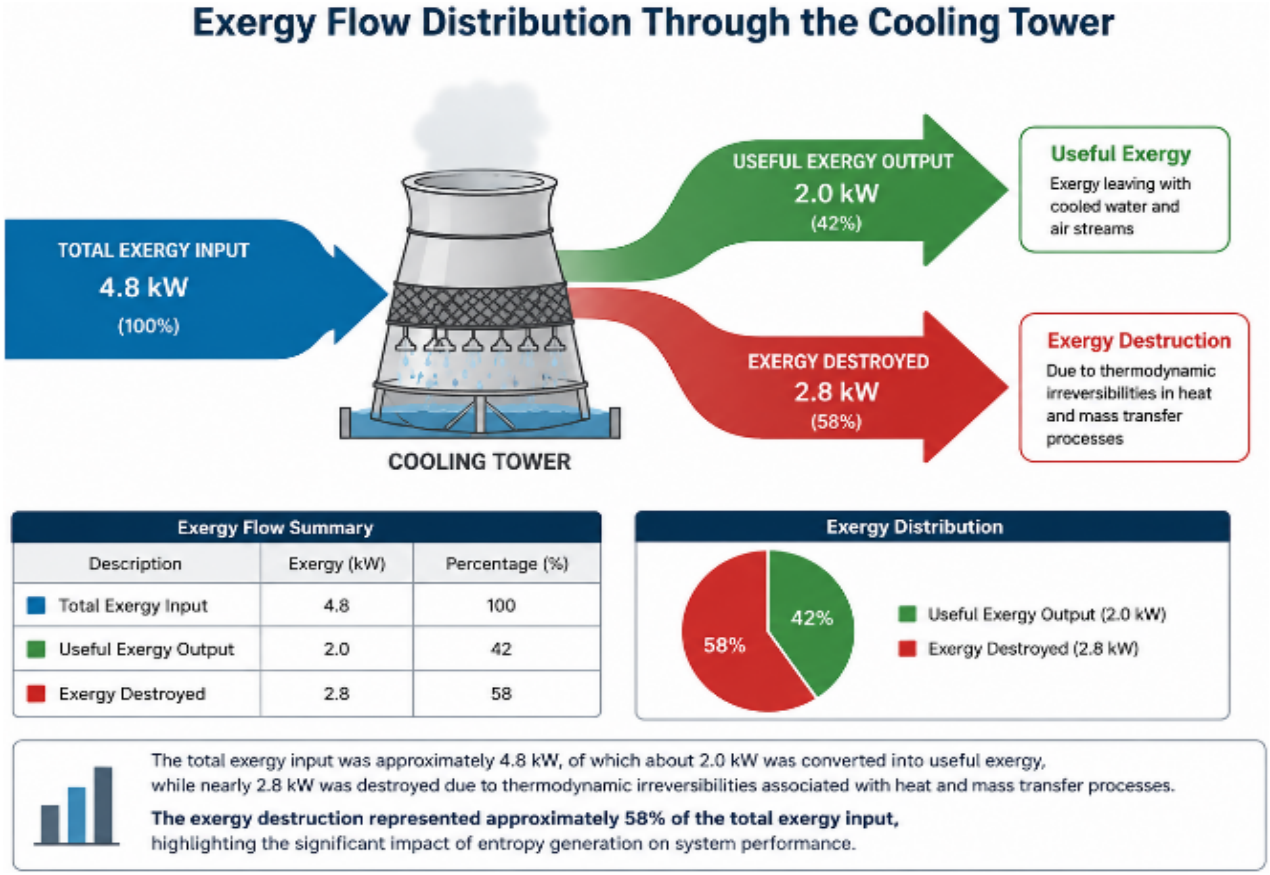


Figure 13. The exergy flow distribution through the cooling tower

Figure 13 illustrates the exergy flow distribution through the cooling tower. The total exergy input was approximately 4.8 kW, of which about 2.0 kW was converted into useful exergy, while nearly 2.8 kW was destroyed due to thermodynamic irreversibility associated with heat and mass transfer processes. The exergy destruction represented approximately 58% of the total exergy input, highlighting the significant impact of entropy generation on system performance.

6. CONCLUSIONS

An integrated experimental, exergy, and annual TRNSYS assessment was conducted for a forced-draft counter-flow wet cooling tower under Iraqi climatic conditions. The principal conclusions and practical engineering implications are given below:

1. Cooling range and thermal efficiency increased with increasing inlet water temperature from 28 to 42 ℃ and water mass flow rate from 0.03 to 0.075 kg/s, getting maximum results of 14.8 ℃ and 74%, respectively.

2. The same operating changes increased the exergy destruction from about 1.0 to 2.8 kW and decreased the exergy efficiency from 57.8% to 11.9%. Therefore, in situations where the most important operation goal is to reject the maximum amount of heat, the inlet water temperature should be maximized together with the flow rate, while medium operating conditions may be more suitable if irreversibility is also an important concern.

3. Annual TRNSYS results revealed that during cooler periods the cooling capacity was about 4.8 kW and it reduced to 1 kW for higher ambient temperature. The wet-bulb temperature should then be considered as a key control variable since it dictates the cooling potential and minimum outlet-water temperature.

4. A higher flow rate can be employed under cooler and drier conditions to take advantage of the greater difference between inlet-water and ambient wet-bulb temperatures and to maximize the cooling capacity. When the cooling load allows, a lower or intermediate water flow rate should be used during hot or humid climates to reduce the driving potential to limit heat and mass transfer, while too high a water loading can increase the exergy destruction without a proportionate increase in useful cooling.

5. The numerical heat-transfer rate was found to be different from the experimental one by about 5.6%, which shows acceptable agreement and can be used to predict annual performance and to do a preliminary selection of operating points under Iraqi climatic conditions when using the validated TRNSYS model.

6. The actual water flow and inlet water temperature should then be adjusted seasonally based on ambient wet-bulb temperature and the desired cooling load in practical operation. The operating point needs to be optimized for both exergy efficiency and thermal efficiency.

ACKNOWLEDGMENT

The authors would like to thank the Technical Engineering College, Baghdad, for their support.

REFERENCES

[1] Naik, B.K., Muthukumar, P. (2017). A novel approach

for performance assessment of mechanical draft wet cooling towers. Applied Thermal Engineering, 121: 14-26. https://doi.org/10.1016/j.applthermaleng.2017.04.042

[2] Xi, Y., Yu, Z.K., Zhang, L., et al. (2023). Research on heat and mass transfer characteristics of a counterflow wet cooling tower using a new type of straight wave packing. International Journal of Thermal Sciences, 193: 108540. https://doi.org/10.1016/j.ijthermalsci.2023.108540

[3] Navarro, P., Ruiz, J., Kaiser, A.S., Lucas, M. (2023). Effect of fill length and distribution on the thermal performance of an inverted cooling tower. Applied Thermal Engineering, 231: 120876. https://doi.org/10.1016/j.applthermaleng.2023.120876

[4] Muangnoi, T., Asvapoositkul, W., Wongwises, S. (2007). An exergy analysis on the performance of a counterflow wet cooling tower. Applied Thermal Engineering, 27(5-6): 910-917. https://doi.org/10.1016/j.applthermaleng.2006.08.012

[5] Ataei, A., Panjeshahi, M.H., Gharaie, M. (2008). Performance evaluation of counter-flow wet cooling towers using exergetic analysis. Transactions of the Canadian Society for Mechanical Engineering, 32(3-4): 499-512. https://doi.org/10.1139/tcsme-2008-0033

[6] Khalifa, A.H. (2015). Thermal and exergy analysis of counter flow induced draught cooling. International Journal of Current Engineering and Technology, 5(4): 2868-2873. http://inpressco.com/category/ijcet.

[7] Akbarpour Ghazani, M., Hashem-ol-Hosseini, A., Emami, M.D. (2017). A comprehensive analysis of a laboratory scale counter flow wet cooling tower using the first and the second laws of thermodynamics. Applied Thermal Engineering, 125: 1389-1401. https://doi.org/10.1016/j.applthermaleng.2017.07.090

[8] Zunaid, M., Murtaza, Q., Gautam, S. (2017). Energy and performance analysis of multi droplets shower cooling tower at different inlet water temperature for air cooling application. Applied Thermal Engineering, 121: 1070-1079. https://doi.org/10.1016/j.applthermaleng.2017.04.157

[9] Kareem, F.A., Al-Dulaimi, M., Lafta, N.S. (2018). Investigation the exergy performance of a forced draft wet cooling tower. International Journal of Engineering and Technology (UAE), 7(4): 2575-2580. https://doi.org/10.14419/ijet.v7i4.16698

[10] Fan, X.C., Lu, X.F., Nie, H., et al. (2021). An experimental study of a novel dew point evaporative cooling tower based on M-cycle. Applied Thermal Engineering, 190: 116839. https://doi.org/10.1016/j.applthermaleng.2021.116839

[11] Ruiz, J., Navarro, P., Hernández, M., Lucas, M., Kaiser, A.S. (2022). Thermal performance and emissions analysis of a new cooling tower prototype. Applied Thermal Engineering, 206: 118065. https://doi.org/10.1016/j.applthermaleng.2022.118065

[12] Qu, J., Li, M., He, C., Zhang, B.J., Chen, Q.L., Ren, J. (2022). Deciphering the optimal exergy field in closed-wet cooling towers using Bi-level reduced-order models. Energy, 238: 121766. https://doi.org/10.1016/j.energy.2021.121766

[13] Li, Y.D., Wu, Y.Y., Zhong, Y., Zhang, S.N. (2024). Numerical study on heat and mass transfer performance of a natural draft wet cooling tower based on baffle optimization. Applied Thermal Engineering, 245: 122738. https://doi.org/10.1016/j.applthermaleng.2024.122738

[14] Chen, X.H., Sun, F.Z., Yang, S.S., Xia, L.J., Zhang, X.Y. (2023). Effect mechanism of wind shields on the thermal performance for mechanical draft wet cooling towers. Applied Thermal Engineering, 219(PA): 119452. https://doi.org/10.1016/j.applthermaleng.2022.119452

[15] Yang, J.C., Gao, M., Wang, M.Y., et al. (2023). Synergistic optimization of partition water distribution, non-equidistant fillings and dry-wet hybrid rain zone for wet cooling towers. Applied Thermal Engineering, 231: 120940. https://doi.org/10.1016/j.applthermaleng.2023.120940

[16] Bueso, M.C., de Nicolás, A.P., Vera-García, F., Molina-García, Á. (2024). Cooling tower modeling based on machine learning approaches: Application to zero liquid discharge in desalination processes. Applied Thermal Engineering, 242: 122522. https://doi.org/10.1016/j.applthermaleng.2024.122522

[17] Qu, X.H., Guo, Q.J., Qi, X.N., Yu, Y. (2024). Numerical and experimental study on performance of seawater cooling towers based on a comprehensive coupling model. Applied Thermal Engineering, 236(PC): 121583. https://doi.org/10.1016/j.applthermaleng.2023.121583

[18] Zhou, C.M., Hu, Y.Y., Zhang, L., et al. (2024). Investigation of heat transfer characteristics of deflected elliptical-tube heat exchanger in closed-circuit cooling towers. Applied Thermal Engineering, 236(PD): 121860. https://doi.org/10.1016/j.applthermaleng.2023.121860

[19] Deng, W.P., Sun, F.Z. (2024). Performance analysis and multi-objective optimization of mechanical draft wet cooling towers based on water saving, plume and cooling characteristics. International Journal of Thermal Sciences, 196: 108656. https://doi.org/10.1016/j.ijthermalsci.2023.108656

[20] Luo, L.C., Guo, P.J., Wang, G. (2025). 3E (energy-exergy-environmental) performance analysis and optimization of seawater shower cooling tower for central air conditioning systems. Processes, 13(5): 1336. https://doi.org/10.3390/pr13051336

[21] Al-Dulaimi, M.J., Kareem, F.A., Hamad, F.A. (2019). Evaluation of thermal performance for natural and forced draft wet cooling tower. Journal of Mechanical Engineering and Sciences, 13(4): 6007-6021. https://doi.org/10.15282/jmes.13.4.2019.19.0475

[22] Wang, L., Li, N.P. (2011). Exergy transfer and parametric study of counter flow wet cooling towers. Applied Thermal Engineering, 31(5): 954-960. https://doi.org/10.1016/j.applthermaleng.2010.11.019

[23] Solar Energy Laboratory, University of Wisconsin-Madison, TRANSSOLAR Energietechnik GmbH, CSTB, Thermal Energy System Specialists (2017). TRNSYS 18: A Transient System Simulation Program-Volume 3: Standard Component Library Overview. Madison, WI, USA. https://sel.me.wisc.edu/trnsys/.

NOMENCLATURE

Cp_a	specific heat of air, kJ/kg·k
Cp_v	specific heat of vapor, kJ/kg·k
Cp_w	specific heat of water, kJ/kg·k
$Ex_{a,c}$	convective heat transfer exergy, kW

$Ex_{a,e}$	evaporative heat transfer exergy, kW
$Ex_{dest.}$	total exergy destruction, kW
Ex_w	exergy of water, kW
$\dot{m}_a$	air flow rate, kg/s
ha	enthalpy of the air, kJ/kg
hf,w	saturated liquid enthalpy of water, kJ/kg
$\dot{m}_w$	water flow rate, kg/s
Q	heat transfer rate, kW
WBT	wet bulb temperature, ℃
R_a	air gas constant, kJ/kg·K
R_v	vapor gas constant, kJ/kg·K
Ta	air temperature, ℃
T_o	dead state temperature, ℃
T_w	water temperature, ℃

Greek letters

η_{ex}	exergy efficiency, %
$\emptyset_o$	relative humidity of the air at dead state temperature
ω	moisture content, kgw/kga

Subscripts

i	inlet
e	exit